

A Neural Network Approach to Predict the Horizontal Air Velocity Component in Low Airspeed Regime

José Márcio Pereira Figueira¹, Donizeti de Andrade² and Ronaldo Vieira Cruz³

^{1,3} Brazilian Institute of Research and Flight Tests ² Technological Institute of Aeronautics, São José dos Campos, SP, Brazil

¹ Master of Science, ² Professor, ³ Doctor

¹ Email: jmpfigueira@hotmail.com

Abstract

The determination of the horizontal air velocity component in low airspeed regime, typically below 40 KIAS, has been a challenge for the rotary-wing engineering development. Regarding this issue, this paper develops a mathematical model, in neural network, for predicting the horizontal air velocity component of the AS 355 F2 helicopter by taking advantage of *Matlab*[®] Neural Network Toolbox, to be used as a real time telemetry tool by Brazilian Institute of Research and Flight Tests, IPEV. By using a flight test acquisition system installed in the AS 355 F2 tail number FAB 8816, some parameters are measured in the fuselage, like stick positions, rotating speeds and attitudes, during steady-state conditions and leveled flight acceleration maneuvers. These measurements are used as input and references to backpropagation neural networks with supervised learning. Two sort of neural networks are developed: one to predict longitudinal air velocity, u , and other to predict the lateral air velocity, v . Training process approach consists of trying and error by changing input parameters set and neural network structure. The Levenberg-Marquardt algorithm is used to perform the optimization process of networks weights and biases. During the validation procedure a new data set is applied to the neural networks that had provided the best training results for each air velocity. It's verified that one longitudinal and lateral neural network association, with 11 input parameters and 2 hidden layers with 25 processing elements each, provides satisfactory results in predicting horizontal air velocity component in stabilized maneuvers, with accuracy level of $\pm 3,4$ kt and $\pm 16^\circ$, along with unsatisfactory results in level flight acceleration maneuvers. Additionally, as a contribution of this work, this neural network association is implemented, by using *Matlab*[®], in the Brazilian Air Command IPEV telemetry facility proving the viability of this computational code as a real-time flight test tool.

Notation

CG = Center of Gravity
 NN = Neural Network
 PE = Processing Element
 R = correlation coefficient
 rb = y -intercept of the best linear regression relating target to neural network output (kt)
 rm = slope of the best linear regression relating target to neural network output
 u = longitudinal air velocity (kt)

u_e = predicted longitudinal air velocity (kt)

v = lateral air velocity (kt)

v_e = predicted lateral air velocity (kt)

V_{ah} = horizontal air velocity component intensity (kt)

V_{ahe} = predicted horizontal air velocity component intensity (kt)

$\sigma_{V_{ah-V_{ahe}}}$ = standard deviation of horizontal air velocity component prediction error (kt)

$\sigma_{\psi_v-\psi_{ve}}$ = standard deviation of sideslip prediction error (kt)

ψ_v = low airspeed sideslip angle ($^\circ$)

ψ_{ve} = predicted low airspeed sideslip angle ($^\circ$)

Introduction

Helicopters are aircraft capable of performing a wide variety of civilian and military missions, such as transport of passengers and/or cargo, medical evacuation, law enforcement, air-to-ground attack, air-to-air attack, reconnaissance, anti-submarine warfare and Search and Rescue.

Although helicopters often operate in airspeed regime over 100 kt, many of these missions may require that a large portion of flight time be conducted in the low speed flight regime, typically below 40 kt [1].

At high airspeeds, the traditional aerodynamic sensor based on pressure differences (pitot-static) provides reliable indications as well as in fixed-wing aircraft. However, these sensors are not able to provide appropriate indications in the low airspeed regime, due to the sensitivity limit of the pitot-static tubes available in the aviation market (above 20 kt), the effects of disturbances and non-linearities of the flow caused by the main rotor inflow and the multiple degrees-of-freedom of the helicopter (vertical, backward and sideward displacements) [2].

In addition to the non-linearities arising from main rotor aerodynamic air flow, other non-linear phenomena increase the difficult in predicting the air velocity, such as:

- possibility of vortex-ring state of the tail rotor when the aircraft is in sideward maneuvering;
- main rotor tip vortices effect on the tail rotor blade; and
- effects of ground vortex created by the main rotor inflow over the airframe in some IGE flight conditions.

Therefore, the helicopter pilots do not have access to air velocity information in hovering flight. These indications are important to, for example:

- maintain the aircraft control margins, considering that it is a flight regime that requires high power level;
- define a safety takeoff profile (outside the high-velocity diagram avoid area);
- define the one engine inoperative safety takeoff profile;
- quantify the attack aircraft weapon system performance;
- develop a warning systems to indicate proximity to hazardous conditions such as vortex-ring state (VRSWS) and
- monitor the fatigue life of aircraft and components, since high vibrations may occur during maneuvers at low airspeeds, such as hovering, steepest approaches, sideward and backward displacements.

It's important to highlight that the vertical air velocity component is provided on board the aircraft, by measuring the temporal variation of static pressure, and generally has a satisfactory accuracy level. Therefore, the problem of estimating the air velocity mentioned above actually refers to the air velocity component related to horizontal plane, or in other words, the horizontal air velocity component.

The development of an accurate way for measuring the horizontal air velocity component has been a challenge since the early rotorcraft aviation. In the 50's, it appears the first low-speed devices, consisting of mounted sensors above the rotor hub of the aircraft [1].

These sensors are based on using two Venturi tubes arranged on opposite sides of a rotating arm and installed above the main rotor hub, as LORAS, *Low Range Airspeed System*. The pressure differential between these two sensors is used to get the horizontal air velocity component of the helicopter [1].

However, this instrument requires means for transferring data captured by the sensor to a fixed reference in the airframe (non-rotating), a fact that requires a fine instrumentation and therefore more expensive devices.

Subsequently, it was created a system called LASSIE, *Low Air Speed Sensing and Indicating System*, capable of allowing the alignment of the pitot tube at 360 degrees with the air flow, providing a measure that is directly related to the horizontal air velocity component [3]. However, this system uses empirical linearization to predict the air velocity components, so that is not capable of providing accurate results.

In addition to these mechanical ways to determine the air velocity vector, there are methods based on other forms of identification different from anemometric way, as numerical or quantitative process, called algorithms.

They are based on real-time measurements of several aircraft's state parameters (for example, pressure altitude, longitudinal and lateral attitudes and control stick positions) and by applying analytical data previously obtained from which it's possible to identify the horizontal air velocity component (intensity and sideslip angle).

The recent application of neural networks approach to predict helicopter low airspeed regime has presented good results. This method is very similar to the algorithm, i.e., several state parameters of the helicopter are measured and there is a process to identify the desired parameter [4].

The main difference is the way to calculate the air velocity. It makes use of neural network technology to determine the correlation between the parameters that direct

affect the system, which may be non-linear, and thus create a calculation methodology, i.e., a mathematical model.

Related to this context, the objective of this work is to develop a validated mathematical model to predict the horizontal air velocity component of the AS 355 F2 aircraft, by using *Matlab*[®] neural network toolbox, for further implementation in the telemetry facility of the Brazilian Institute of Research and Flight Tests - IPEV.

Identification Process of the Horizontal Air Velocity Component

Flight Testing Performed

The data used for training and validating the neural networks of this work are obtained in 5 hours and 45 minutes of low airspeed flight test shared into three flights, with three different Take Off Weights, all performed in São José dos Campos airfield - Brazil, on a instrumented AS 355 F2 aircraft, tail number FAB 8816, belonging to the IPEV fleet.

The aircraft is flight tested in stabilized horizontal air velocity component, both IGE and OGE conditions, by using the pace car method.

All the flights are performed with no doors opened and Automatic Pilot disengaged.

Figure 1 shows a picture of the flight test carried out.



Figure 1 - Picture of Pace Car Flight Test Method.

The method used to define IGE and OGE conditions is the external reference, in which stabilized test points are performed by the test pilot keeping the vertical ground reference, when in hover, and with the help of external references to maintain the height, during relative aircraft-ground displacement.

In addition, longitudinal level flight accelerations to simulate normal take off profile are performed, starting from hovering, also using the help of external references to maintain the height.

It is used the low airspeed sideslip angle definition presented in Figure 2.

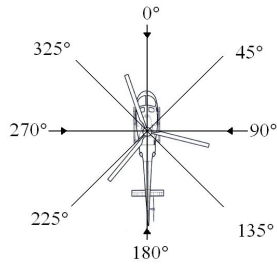


Figure 2 - Notation of the Low Airspeed Sideslip Angle, ψ_s .

The helicopter horizontal air velocity component is determined by recording the horizontal ground speed provided by DGPS installed in the aircraft with 2 Hz sample rate. For this, the completion of the test points is restricted to wind intensity less than 5 kt. The actual wind conditions (intensity and direction) were measured during the flight tests, resulting in $2,3 \pm 1,1$ kt, and, consequently, an uncertainty level of 3,4 kt on the DGPS horizontal air velocity.

Training and Validation Data Sets

According to McCool & Hass [1] and Goff [5], the selection of neural network of set data is crucial to the success of this tool. In addition, it should be used two data sets during the development phase: one for training and another to validate the neural network model.

The training set should consist of representative points of the whole flight envelope in which the network model is intended to be used, i.e., at least combinations of weight, environment conditions, horizontal air velocity and low airspeed sideslip angle must be tested.

Additionally, factors that can significantly affect the relationship between input and output parameters should be considered and analyzed to select the data set. For example, McCool & Hass [1] and Samlioglu [6] indicated that the ground effect affects the results of neural networks, due the high aerodynamic level of change between IGE and OGE conditions.

Therefore, the stabilized test points are divided into two data sets, training and validation, as presented in the polar plots (Figures 3 to 5). These sets selection process are based on the idea of defining a set of training data that better represents flight tested domain and also different ground effect conditions.

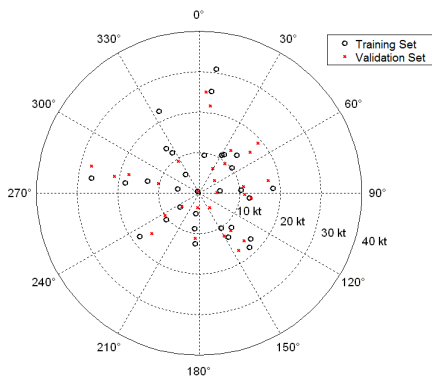


Figure 3 – IGE Stabilized Average Points of Training and Validation Sets Obtained in Flight 1.

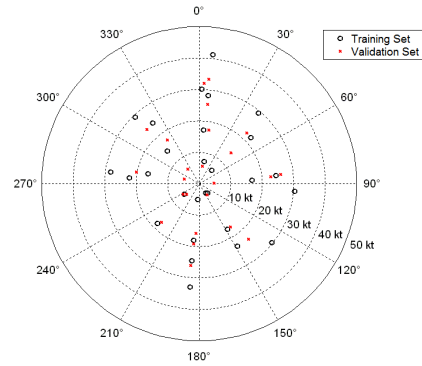


Figure 4 – IGE Stabilized Average Points of Training and Validation Sets Obtained in Flight 2.

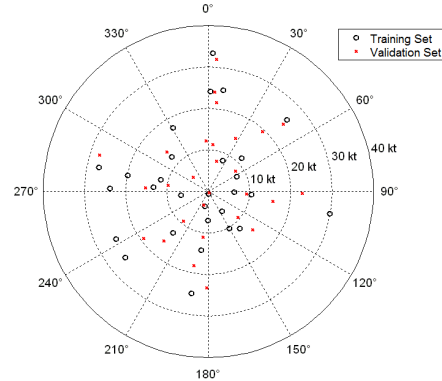


Figure 5 – OGE Stabilized Average Points of Training and Validation Sets Obtained in Flight 3.

These two data sets, whose averages are presented in Figures 3 to 5, represent the total number of sampled points shown in Table 1.

Table 1: Samples Number of Stabilized Test Points for Training and Validating Data Sets.

| Data Set | Flight Condition | Number of Stabilized Points | Number of Samples |
|------------|------------------|-----------------------------|-------------------|
| Training | IGE | 60 | 2195 |
| | OGE | 31 | 782 |
| | Total | 91 | 2977 |
| Validation | IGE | 54 | 1742 |
| | OGE | 28 | 629 |
| | Total | 82 | 2371 |

As performed to stabilizing test points, the longitudinal level flight accelerations are also divided into training and validation sets.

Figures 6 to 10 present the horizontal air velocity components, longitudinal and the lateral, u and v respectively, selected to training and validation data set.

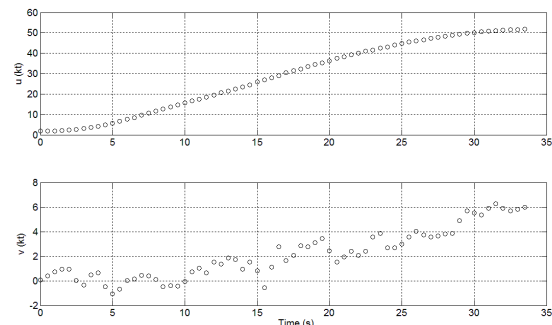


Figure 6 – IGE Level Flight Acceleration of Training Database Set Obtained on Flight 2.

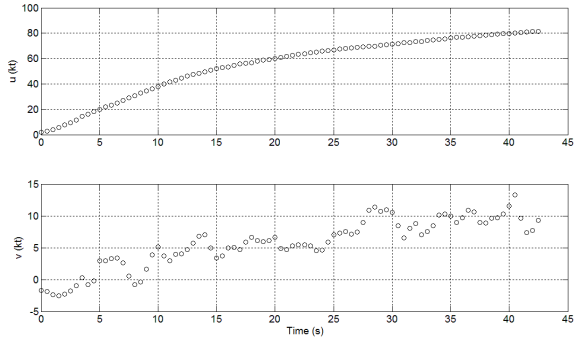


Figure 7 – Second IGE Level Flight Acceleration of Training Database Set Obtained on Flight 2.

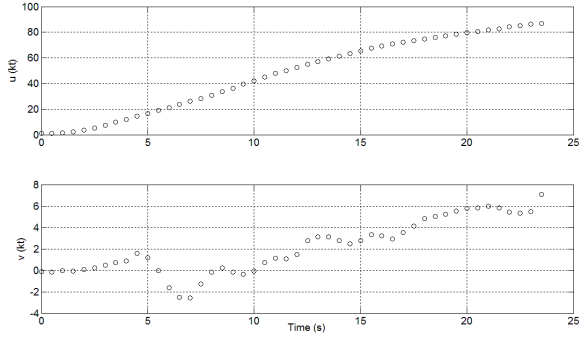


Figure 8 – OGE Level Flight Acceleration of Training Database Set Obtained on Flight 3.

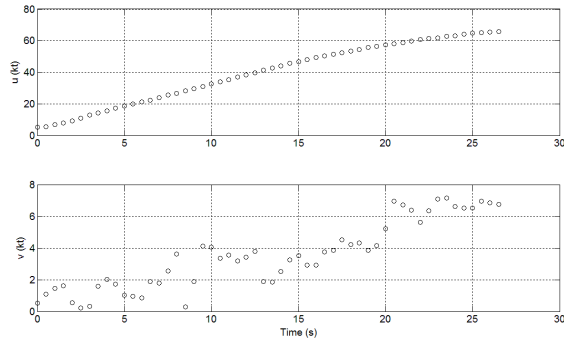


Figure 9 – IGE Level Flight Acceleration of Validation Database Set Obtained on Flight 2.

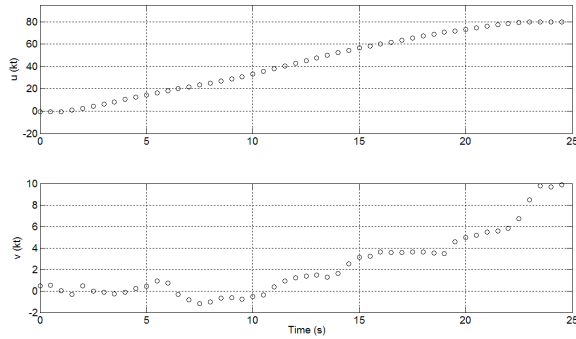


Figure 10 – OGE Level Flight Acceleration of Validation Database Set Obtained on Flight 3.

The total amount of samples of longitudinal level flight acceleration is 202 points, for training data set, and 102 points for validation data set.

Neural Network Model

The networks input parameters selected for this study of predicting the horizontal air velocity component by neural network are presented in Table 2.

Table 2:
Neural Network Input Parameters.

| # | Parameter |
|----|--|
| 1 | Ddc , collective stick position (%) |
| 2 | Ddl , lateral cyclic stick position (%) |
| 3 | Ddm , longitudinal cyclic stick position (%) |
| 4 | Ddn , pedal position (%) |
| 5 | θ , pitch attitude ($^{\circ}$) |
| 6 | ϕ , roll attitude ($^{\circ}$) |
| 7 | p , roll rate ($^{\circ}/s$) |
| 8 | q , pitch rate ($^{\circ}/s$) |
| 9 | r , yaw rate ($^{\circ}/s$) |
| 10 | Tq , engines torque (%) |
| 11 | W , helicopter gross weight (kgf) |
| 12 | Nr , main rotor RPM (rpm) |
| 13 | Xcg , longitudinal CG position (m) |

Based on these thirteen input parameters presented in Table 2, three input sets are defined:

- Set 1: Ddc , Ddl , Ddm , Ddn , θ , ϕ , p , q , r e Tq ;
- Set 2: Set 1 with addition of W ; and
- Set 3: Set 1 with addition of W , Nr e Xcg .

These sets are defined based on McCool & Hass [1] and Goff [5] previous results and on the parameters acquired by the flight test acquisition system of FAB 8816 aircraft.

The first set, containing 10 parameters, is favorable for a real time onboard application, regarding that all parameters are obtained directly from the flight instrumentation bus, i.e., it is not necessary to insert any additional aircraft pre start up conditions, as in the case of W and Xcg parameters.

The main rotor RPM, Nr , was removed from set 1 because of its small variation during the flight, as the aircraft provides an automatic control of it. Moreover, the results presented by Goff [5] shows low contribution of the Nr variation in the prediction of the horizontal air velocity component.

Set 2 represents the set 1 plus the parameter W , which is easily derived from the amount of remaining fuel in the tanks, but still needs the insertion of the initial condition of *Zero Fuel Weight*.

Set 3, containing 13 parameters, is the data set that has provided the best results, in McCool & Hass [1] work, to predict the horizontal air velocity component.

Neural Networks Architecture

Analogous to Goff [5], two neural networks are built: one to estimate the longitudinal air velocity, u , and one to the lateral air velocity, v .

By means of the vector sum of the predicted longitudinal and lateral air velocity components by neural network is possible to determine the predicted horizontal air velocity component (Figure 11).

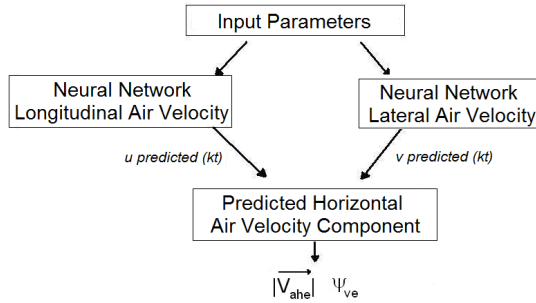


Figure 11 – Schematics of Neural Network Approach to Predicting the Horizontal Air Velocity Component of the AS 355 F2 in Low Airspeed Regime.

In Figure 11, V_{ahel} is the predicted horizontal air velocity component intensity (kt); and ψ_{ve} is the predicted low airspeed sideslip angle ($^{\circ}$).

Based on McCool & Hass [1] and Samlioglu [6] prediction results, this paper uses the *backpropagation* algorithm approach to predict the intensity of horizontal air velocity components. In addition, to produce a faster and more efficient optimization process of NN weights and biases, the *Levenberg-Marquardt* algorithm is used.

It's important to highlight that the predicted low airspeed sideslip angle is obtained indirectly, since it is the combination of predicted longitudinal and lateral air velocity components, u_e and v_e respectively. Therefore, the signs of u_e and v_e define direction, while their intensities determine the predicted horizontal air velocity component.

Neural Networks Training Process

The definition of optimal neural network architecture to predict the longitudinal and lateral air velocity components is performed by trying and error, by modifying the input database (ground effect, stabilized and non-stabilized flight condition), the input data set, the number of hidden layers, the transfer function (or activation functions) and the number of Processing Elements per layer.

The whole training process is conducted using the *backpropagation* neural network with *Levenberg-Marquardt* optimization existing on *Neural Network Toolbox of Matlab[®]*.

The NN architecture is changed, during the training process, according to:

- Input database (stabilized IGE, stabilized OGE and level flight acceleration);
- Input data set (1, 2 and 3);
- Number of PE per layer (15, 25 and 35); and
- Transfer function of hidden layers (*tansig*, *logsig* and *radbas*).

During the training process it is noted that the increase in the number of PE and hidden layers increase the requested processing time for the same number of iterations. However, this change provides better adherence to the required longitudinal and lateral air velocity components output values. The maximum number of PE per hidden layer is 35, since the computational code takes about 20 minutes to run just one iteration over this PE value, in the case of an *Intel[®] CoreTM 2 Duo CPU T5800 2.00 GHz, 4.00 GB RAM* processor.

Additionally, it is verified that two hidden layers and 25 PE per layer network architecture present, in general, the best trade off between number of iterations, time and prediction quality. As a consequence of this observation, this work gives special attention to this neural network architecture during the trying and error training process.

As statistical analysis tool for evaluating the training results of longitudinal and lateral air velocity networks is used:

- the standard deviation of the prediction error, and
- the linear regression between the measured air velocity components and the output predicted by using neural networks approach.

At the linear regression, a perfect fit corresponds to a unitary slope, i.e., $rm = 1$, intercepting zero, i.e., $rb = 0$. Thus, these neural network results would indicate a perfect mapping of the desired output.

Additionally, the correlation coefficient, R , is a measure of the relationship level between two parameters. In the case of linear regression it corresponds to the measure of how linear is the relationship between the predicted longitudinal and lateral air velocity components and their actual values measured in flight. If this coefficient is equal to 1, it indicates a perfect linear correlation between network output and desired one.

About the different transfer functions used for training the networks to predict the longitudinal air velocity component, it is noted that the best results, maintaining other NN architecture parameters constant, both in terms of standard deviation of the prediction error and of linear regression, are obtained for networks trained with the *tansig* transfer function. On the other hand, it is not observed any higher performance transfer function to predicting lateral air velocity component.

Similarly to the results presented in the work of McCool & Hass [1] and Samlioglu [6], it is noted that, taking the same network architecture, a better prediction match for the networks trained with OGE stabilized database is reached then for the networks trained with IGE database. This fact is justified by the inherent nonlinearities aerodynamic conditions caused by the proximity of the aircraft with the ground, which complicate the building of neural networks logical connections and therefore, the learning process.

To predict the two horizontal air velocity components, in general, the standard deviation of the prediction error is ranged between 0,4 kt and 1,7 kt, with a correlation coefficient above 98% when accounting the NN architecture of two hidden layers, 25 PE per layer and input database derived from stabilized conditions (IGE and OGE) and level flight accelerations up to 40 kt.

As for the horizontal air velocity components, measured by the DGPS during flight tests of this study (they have uncertainty of $\pm 3,4$ kt) it is used this value as a reference of training process quality. Therefore, the prediction results with standard deviation of prediction error below the flight test uncertainty is considered satisfactory.

By this analysis, it is selected the longitudinal and lateral neural networks that have reached satisfactory standard deviation for the prediction error, obtained

good linear regression results, and whose input database came from a diversity of flight conditions (stabilized and non-stabilized).

Based on these premises, the longitudinal and lateral air velocity components trained neural networks chosen for validation step are given in Tables 3 and 5, respectively. All the networks selected have two hidden layers. In addition, it is presented their training statistical results on Tables 4 and 6.

Table 3:
Longitudinal Air Velocity Component NN Trained and Selected for Validation Process.

| Longitudinal NN | Training Input Database | Data set | # PE | Transfer function |
|-----------------|--|----------|------|-------------------|
| #1 | Stabilized IGE and OGE | 1 | 25 | Tansig |
| #2 | | 1 | 25 | Radbas |
| #3 | | 1 | 35 | Tansig |
| #4 | | 3 | 25 | Tansig |
| #5 | | 2 | 25 | Tansig |
| #6 | Stabilized OGE | 1 | 25 | Tansig |
| #7 | Stabilized IGE | 3 | 25 | Logsig |
| #8 | Stabilized IGE, stabilized OGE and level flight acceleration up to 40 kt | 1 | 25 | Logsig |
| #9 | | 1 | 25 | Radbas |
| #10 | | 2 | 25 | Logsig |
| #11 | | 2 | 25 | Radbas |

Table 4:
Training Results of the Longitudinal Air Velocity Component NN Selected for Validation Process.

| Longitudinal NN | σ_{u-ue} (kt) | rm | $rb.10^{-2}$ (kt) | R |
|-----------------|----------------------|-------|-------------------|-------|
| #1 | 1,01 | 0,993 | 1,11 | 0,997 |
| #2 | 1,24 | 0,990 | 1,60 | 0,995 |
| #3 | 1,04 | 0,993 | 1,21 | 0,997 |
| #4 | 0,70 | 0,997 | 0,55 | 0,998 |
| #5 | 1,00 | 0,994 | 1,12 | 0,997 |
| #6 | 1,00 | 0,994 | 1,12 | 0,997 |
| #7 | 0,76 | 0,997 | 0,73 | 0,998 |
| #8 | 1,41 | 0,988 | 2,66 | 0,994 |
| #9 | 1,16 | 0,992 | 1,81 | 0,996 |
| #10 | 1,15 | 0,992 | 1,78 | 0,996 |
| #11 | 1,90 | 0,977 | 5,12 | 0,989 |

Table 5:
Lateral Air Velocity Component NN Trained and Selected for Validation Process.

| Lateral NN | Training Input Database | Data set | # PE | Transfer function |
|------------|--|----------|------|-------------------|
| #1 | Stabilized IGE and OGE | 1 | 25 | Tansig |
| #2 | | 1 | 25 | Radbas |
| #3 | | 1 | 35 | Tansig |
| #4 | | 3 | 25 | Tansig |
| #5 | Stabilized OGE | 1 | 25 | Logsig |
| #6 | Stabilized IGE | 1 | 25 | Tansig |
| #7 | Stabilized IGE, stabilized OGE and level flight acceleration up to 40 kt | 1 | 25 | Logsig |
| #8 | | 1 | 25 | Radbas |
| #9 | | 2 | 25 | Tansig |

Table 6:
Training Results of the Lateral Air Velocity Component NN Selected for Validation Process.

| Lateral NN | σ_{u-ue} (kt) | rm | $rb.10^{-2}$ (kt) | R |
|------------|----------------------|-------|-------------------|-------|
| #1 | 1,14 | 0,991 | -0,79 | 0,995 |
| #2 | 1,31 | 0,988 | -0,99 | 0,994 |
| #3 | 1,20 | 0,990 | -0,82 | 0,995 |
| #4 | 0,77 | 0,996 | -0,33 | 0,998 |
| #5 | 0,80 | 0,995 | -0,96 | 0,998 |
| #6 | 0,90 | 0,994 | -0,25 | 0,997 |
| #7 | 1,13 | 0,991 | -0,72 | 0,995 |
| #8 | 1,09 | 0,991 | -0,71 | 0,995 |
| #9 | 0,81 | 0,995 | -0,35 | 0,998 |

Neural Networks Validation Process

By introducing the input database selected for the validation process, divided in flight conditions, in the neural networks chosen in the previous step, it is obtained the predicted longitudinal and lateral air velocity components, u_e and v_e respectively.

Tables 7 and 8 present the longitudinal and lateral air velocity components networks results that have presented the best performance during the validation process.

Table 7:
Results of Longitudinal Air Velocity Component NN Validation Process.

| u NN | Validation Input Database | σ_{u-ue} (kt) | rm | $rb.10^{-2}$ (kt) | R |
|------|--|----------------------|-------|-------------------|-------|
| #8 | Stabilized IGE and stabilized OGE | 4,47 | 0,973 | -11,79 | 0,937 |
| | Stabilized IGE, stabilized OGE and level flight acceleration up to 40 kt | 4,54 | 0,962 | -11,85 | 0,936 |
| | Stabilized IGE, stabilized OGE and whole level flight acceleration data | 6,53 | 0,809 | -3,04 | 0,901 |
| #10 | Stabilized IGE and stabilized OGE | 3,38 | 1,039 | -5,12 | 0,967 |
| | Stabilized IGE, stabilized OGE and level flight acceleration up to 40 kt | 3,43 | 1,037 | -5,63 | 0,967 |
| | Stabilized IGE, stabilized OGE and whole level flight acceleration data | 5,29 | 0,882 | 3,66 | 0,936 |

Table 8:
Results of Lateral Air Velocity Component NN Validation Process.

| v NN | Validation Input Database | σ_{u-ue} (kt) | rm | $rb.10^{-2}$ (kt) | R |
|------|--|----------------------|-------|-------------------|-------|
| #8 | Stabilized IGE and stabilized OGE | 3,83 | 0,892 | 17,45 | 0,925 |
| | Stabilized IGE, stabilized OGE and level flight acceleration up to 40 kt | 3,83 | 0,892 | 15,08 | 0,924 |
| | Stabilized IGE, stabilized OGE and whole level flight acceleration data | 3,93 | 0,885 | 4,11 | 0,918 |
| #9 | Stabilized IGE and stabilized OGE | 3,53 | 0,963 | 26,67 | 0,940 |
| | Stabilized IGE, stabilized OGE and level flight acceleration up to 40 kt | 3,54 | 0,962 | 25,52 | 0,939 |
| | Stabilized IGE, stabilized OGE and whole level flight acceleration data | 3,59 | 0,959 | 18,24 | 0,936 |

Based on the validation results previously shown, the longitudinal NN #10 and lateral NN #9 have been validated to predict the horizontal air velocity components of the AS 355 F2 aircraft, since they provide estimation error results within the measurement uncertainty of the flight tests data.

It is important to highlight that these two selected longitudinal and lateral networks were trained by using input data Set 2. Thus, there is the necessity of introducing the *Zero Fuel Weight* value at the beginning of the test flight, so that the prediction process may occur.

Predicted Horizontal Air Velocity Component

As shown in Figure 11, from the predicted values of longitudinal and lateral air velocity components, by vector sum, the horizontal air velocity component (magnitude and direction) can be determined.

Table 9 presents the standard deviation of horizontal air velocity component prediction error, $\sigma_{V_{ah}-V_{aeh}}$, and standard deviation of sideslip prediction error, $\sigma_{\psi_{lv}-\psi_{lve}}$, the horizontal air velocity component and the linear regression results from the neural network association that has reached the best performance level.

Table 9:
Horizontal Air Velocity Component Results in Validation Process.

| NN | | Validation Input Data | Horizontal Air Velocity Component Intensity | | | | $\sigma_{\psi_{lv}-\psi_{lve}}$ (°) |
|----------|----------|---|---|-----------|----------------|----------|-------------------------------------|
| <i>u</i> | <i>v</i> | | $\sigma_{V_{ah}-V_{aeh}}$ (kt) | <i>rm</i> | <i>rb</i> (kt) | <i>R</i> | |
| # 10 | # 9 | Stabilized IGE and OGE | 3,29 | 1,026 | 0,152 | 0,922 | 10,2 |
| | | Stabilized IGE and OGE, and level flight acceleration up to 40 kt | 3,34 | 1,022 | 0,206 | 0,922 | 10,3 |
| | | Stabilized IGE and OGE and whole level flight acceleration data | 5,27 | 0,761 | 3,656 | 0,862 | 10,2 |

The prediction accuracy level of the low airspeed sideslip angle is only assessed by the standard deviation of the prediction error, because the linear regression of a cyclical scale is distorted at the edges, which makes difficult to apply the linear regression method.

Figures 12 to 14 present the linear regression results of longitudinal NN #10 and lateral NN #9 association. For all these figures the database input consists of stabilized IGE, stabilized OGE and level flight acceleration data up to 40 kt.

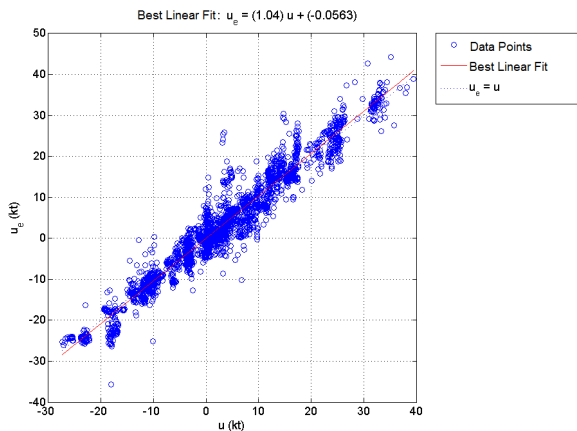


Figure 12 – Linear Regression Analysis of Longitudinal Air Velocity Predicted by NN #10 in the Validation Process.

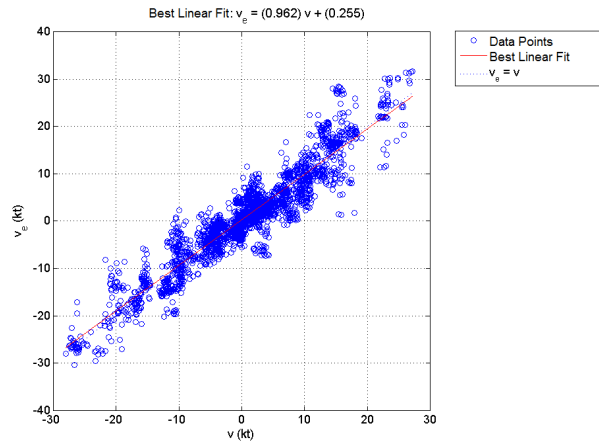


Figure 13 – Linear Regression Analysis of the Lateral Air Velocity Predicted by NN #9 in Validation Process.

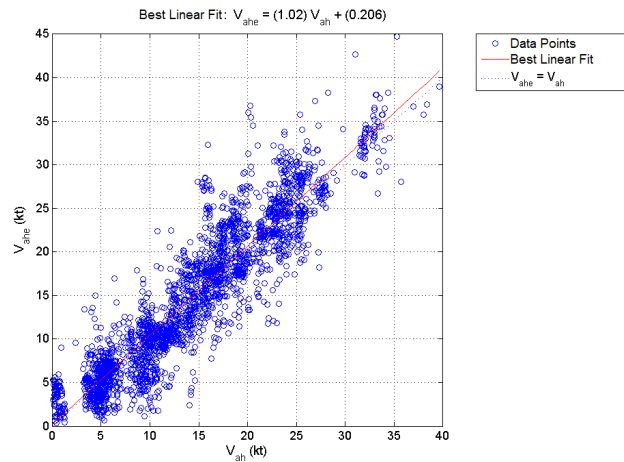


Figure 14 – Linear Regression Analysis of Horizontal Air Velocity Predicted by Longitudinal NN #10 and Lateral NN #9 Association and Validation Data Set.

As the uncertainty of the flight test data is $\pm 3,4$ kt, based on the wind recorded during the flights, the results presented in Table 8 show that the magnitude of the predicted horizontal air velocity component has satisfactory values of standard deviation of the prediction error for stabilized database. This remark is also valid for non-stabilized conditions (level flight acceleration limited to 40 kt).

It is noted that the addition of level flight accelerations samples above 40 kt range increases the standard deviation of the prediction error. As the database used for training process, to all validated neural networks architecture, is restricted to stabilized and non-stabilized points below 40 kt, the accuracy level provided by NN for mapping the air velocity components above 40 kt is degraded whenever out of the training airspeed envelope.

Regarding linear regression results, the intensity of the horizontal air velocity component shows high correlation coefficient values (greater than 0,9) for stabilized and non-stabilized limited to 40 kt input database. Moreover, this NN association presents satisfactory levels of slope and y-intercept point.

From Table 9 one observes that the uncertainty level reached by the predicted low airspeed sideslip angle is not direct dependent of the training database

envelope, such as noted with the intensity error. This happens because the level flight accelerations were performed only in forward direction, since the goal is to identify the horizontal air velocity component during a normal takeoff procedure. Therefore, the non-stabilized database used for training and validation process present the same sideslip angle envelope (around zero degrees).

In conclusion, the longitudinal NN #10 and lateral NN #9 association provides satisfactory results to predict the horizontal air velocity component of AS 355 F2 in low airspeed stabilized and level flight acceleration below 40 kt conditions, with an uncertainty level of $\pm 3,4$ kt and $\pm 16^\circ$.

Additionally, in the event of any change in the flight test acquisition system installed onboard FAB 8816 aircraft or the Automatic Pilot assistance during flight, it is recommended to perform new low airspeed flight tests to verify the reliability and the prediction performance of the neural networks association validated in this work. If the results show unacceptable degradation prediction performance, the same procedures presented in this paper shall be followed to obtain the networks that best fit the changes.

Implementation in a Telemetry Facility

To confirm the feasibility of using the validated longitudinal NN #10 and Lateral NN #9 association in the Brazilian Institute of Research and Flight Tests a computational code to predict the horizontal air velocity component, in *Mallab*[®] is implemented at its flight test facility.

This predicting code is installed in parallel with telemetry facility internal network to provide horizontal air velocity component prediction following the instrumentation data reception, data reading and calculations estimates in real time. Figure 15 presents the telemetry user interface implemented.

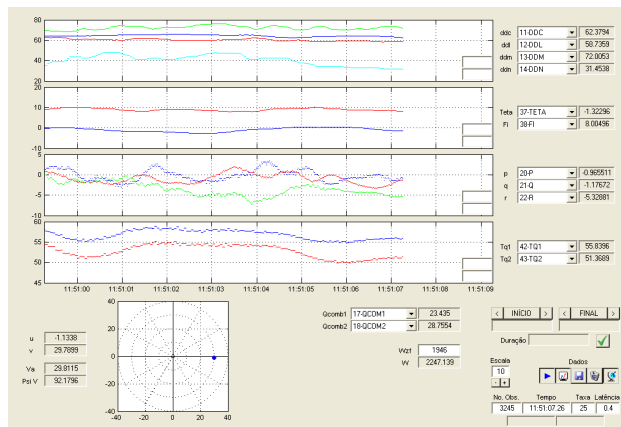


Figure 15 – Telemetry User Interface to Predicting the Horizontal Air Velocity Component of the AS 355 F2 in Low Airspeed Regime.

It is important to highlight that the polar diagram presented in the bottom left side of Figure 15 is a pictorial representation of the real time predicted horizontal air velocity component and its longitudinal and lateral components predictions, which are presented in the abscissa and ordinate axes, respectively. The small blue circle presented on the polar diagram corresponds to the predicted horizontal air velocity component and the before flight input of *Zero Fuel Weight* value is inserted in the bottom right box of the screen (label W_{zf}).

As the flight test acquisition system installed in AS 355 F2, tail number FAB 8816, has been removed from the aircraft just after the three flight tests conducted for this study, and all recorded data are run on the telemetry facility. Thus, simulation data have been received in real time and the validated NN computational code verified.

In no time of these simulations is verified data reception failure or prediction processing interruption.

At stabilized conditions, either for IGE or OGE, the horizontal air velocity components indications are stable and within low intensity oscillation range. This prediction characteristic provides enough tools to allow the pilot to stabilize the aircraft by using this information.

In predicting horizontal air velocity component intensity below 10 kt, due the fact that the magnitude level be around the NN prediction uncertainty ($\pm 3,4$ kt), it is noted that small u_e and v_e perturbations may turn difficult the use of predicted low airspeed sideslip angle indication to stabilize the aircraft.

Through the use of this feature at the telemetry facility, it is verified that the application of horizontal air velocity component prediction indication for non-stabilized maneuvers is unsatisfactory, probably mainly due to the fact that the predicted time varying maneuver is neither gradual nor progressive, during the whole level flight acceleration maneuver.

In this regard, it has been identified accumulative predictions around 0 kt, at the beginning of the maneuver, and close to 40 kt, at the end of maneuver, as shown in Figure 16. Such behavior is an obstacle to perform this sort of maneuver by following the predicted air velocity components indications of the mathematical model presented in this work.

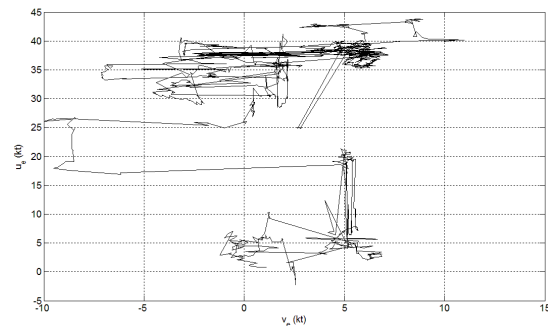


Figure 16 – Example of Polar View Presented to the Pilot for a Complete Time Varying Predicted Level Flight Acceleration.

In general, these features are observed in all run level flight accelerations, regardless whether IGE or OGE. Thus, the use of the results of this work in this kind of maneuver, despite the uncertainty prediction level achieved during the validation process, is unsatisfactory in trials requiring such information to maintain the acceleration rate.

Conclusions and Recommendations

In this work a neural network mathematical model to predict the horizontal air velocity component for AS

355 F2 helicopter, through the use of existing *Matlab*[®] neural networks toolbox, is validated.

It's verified that one longitudinal and lateral *backpropagation* neural network association, with 11 input parameters ($Ddl, Ddm, Ddn, Ddc, \theta, \phi, p, q, r, Tq$ e W), and two hidden layers with 25 processing elements each, provides satisfactory results in predicting horizontal air velocity component in stabilized maneuvers, with accuracy level of $\pm 3,4$ kt and $\pm 16^\circ$. Unsatisfactory results are observed in level flight acceleration maneuvers due to the effect of time varying prediction points accumulation.

In addition, the implementation of the results of this work in the telemetry facility of IPEV is performed and considered feasible. Besides, it encourages further studies of the applicability of predicting the horizontal air velocity component in test flights of performance and handling qualities of the IPEV's Flight Test Course syllabus.

Suggestions for further investigations following this research include:

- increase the amount of training database for training the neural networks process and introduce the helicopter angular accelerations as input parameters of these networks, in order to improve the non-stabilized prediction performance;
- verify the suitability of using, in real time, the computational code implemented in IPEV's telemetry facility in hovering testing performance flight, vertical climb performance, level flight performance, height-velocity diagram tests and to determine the Category A takeoff profile on the Brazilian Flight Test Course syllabus;
- verify the suitability of using, in real time, the computational code implemented in IPEV's telemetry facility to implement new flight test techniques to determine the most critical conditions for entry into vortex-ring state for AS 355 F2 aircraft; and
- implement this computational code onboard of AS 355 F2 flight test instrumented aircraft, by using notebook, and verify the suitability of its application as an horizontal air velocity component indicator to be used by pilots during performance and handling qualities flights at the IPEV's Flight Test Course.

References

- [1] MCCOOL, K. M.; HASS, D.J; SCHAEFER; C.G. JR, A **Neural network based approach to helicopter low airspeed and sideslip angle determination**. AIAA Flight Simulation Technologies Conference, San Diego, July 29-31, 1996.
- [2] HASSENPFUG, W; SCHWÄBLE, R.. **Method for determining the horizontal airspeed of helicopter in low speed ranges**. United States Patent 4.702.106. Germany, Oct. 1987.
- [3] MCCUE, J.J. **Pitot-static Systems**. US Naval Test Pilot School. USA: Patuxent River, 1994. Chapter Nine.
- [4] KNIGHT, C.G. **Low Airspeed Measuring Devices for Helicopter Usage Monitoring Systems**. Austrália: DSTO Platforms Sciences Laboratory, 2003

[5] GOFF, D.A; THOMAS, S.M.; JONES, R.P.; MASSEY, C.P. **A neural network approach to predicting airspeed in helicopters**. Neural Computing & Applications, London. 2000.

[6] SAMLIOGLU, O. **A neural network approach for helicopter airspeed prediction**. California, USA: Naval Postgraduate School, 2002.